Non-Parametric Multi-Target Data Association and Tracking for Multistatic Radars

S. Sruti and K. Giridhar

***Abstract*— Multistatic radar systems provide better detection performance for stealth airborne platforms and are resilient to single-point failures. However, when multiple targets are present over the radar surveillance region, incorrect target associations to the measurements could create ghost targets. Computationally efficient and accurate de-ghosting and tracking multiple targets are critical tasks in real-time distributed radar systems. By exploiting the geometry of the measurement model in the association process, we propose a novel and efficient data association approach followed by a tracking algorithm in this work. It utilizes the Time-of-Arrival and bistatic Doppler frequency measurements of the targets with respect to different transmitter-receiver pairs to accurately determine and track the 3D positions and velocities of the targets. The proposed approach is non-parametric as it does not need any assumption on the initial states or the number of targets and their motion models, but only uses the knowledge of the geometry of the terrestrial radar sensors. This Non-Parametric Data Association and Tracking (NPDAT) algorithm is tested with multiple targets in two significant scenarios: (i) all the targets are simultaneously present in the region, and (ii) targets arrive and depart the region based on a random arrival pattern. Our approach precisely tracks targets even during cross-over and also tracks fast-maneuvering targets. This NPDAT algorithm is compared with popular existing methods and is shown to exhibit superior performance in estimation accuracy and maneuvering target tracking ability, even while enjoying a significantly lower time and implementation complexity.**

***Index Terms*— Data association, De-ghosting, Geometrical approach, Localization, Multistatic radar, Multi-target tracking**

I. Introduction

THE motivation for a distributed radar includes detection and tracking of low Radar Cross Section (RCS) maneuvering targets, counteracting anti-radar tactics and overcoming single-point failure. Multistatic radar with widely separated transmitters and receivers [1] achieves superior performance over conventional monostatic radars due to large area coverage and inherent spatial diversity.

Multi-target data association and tracking are critical tasks in a multistatic radar system. It involves estimating the number of targets and their states and tracking them at successive intervals from a noisy and cluttered set of observations. The challenges associated with Multi-Target Tracking (MTT) are the time-varying number of targets, false measurements, misdetections, track initiation and management, data association, and clutter. Several algorithms available in open literature address the problem of MTT and data association. Many probabilistic approaches exist but are rarely used in practice due to their complexity and assumptions on the number of targets and their motion models. Techniques that handle maneuvering target tracking are intricate and pose challenges for real-time implementation. Commonly, in tracking context, data association is performed using prior knowledge from the target's state model, usually involving either "soft" association based on probabilistic association [2] or "hard" association based on assignment techniques [3]. There exist other approaches that do not need explicit associations, such as Random Finite Sets (RFS) [4] and Symmetric Measurement Equations (SME) [5].

Target tracking is accomplished through explicit data association in techniques like Nearest Neighbours (NN), Multiple Hypothesis Tracking (MHT) [6], multi-target Particle Filter (PF) [7] and Probabilistic Data Association (PDA) [8]. At each time step in NN, a single nearest measurement is associated with each target by assuming all other measurements are generated from clutter. MHT carries forward all the association hypotheses to the next time-step and aggregates them over time. The best possible hypothesis for the previous time is evaluated in retrospect [6]. The PDA framework is an all-neighbor data association method that associates based on the likelihood of measurements to each target.

These data association-based algorithms are invariably combinatorial in nature and suffer from an exponential increase in computational complexity as the number of targets increases. Recently, the Probability Hypothesis Density (PHD) filter based on the RFS framework [4] and Bayesian analysis has gained significant interest in MTT for problems involving many targets. Multisensor MTT cannot be derived as a simple extension from the single-sensor case owing to the added uncertainties in track formation, track maintenance and track-to-track association [9]. The mathematical structure of the optimal solution for multi-sensor MTT is well analyzed in [10]. However, the optimal solution to the multi-sensor MTT problem using a recursive Bayes filter is computationally intractable [11]. It is well established that the data association-based algorithms such as Global NN (GNN), MHT and Joint PDA (JPDA) [12] suffer from a prohibitively high computational cost in a multi-sensor model. In PF-based algorithms, it becomes necessary to propagate a large number of particles to avoid sample impoverishment, rendering these methods nearly practically infeasible [13]. Even for the RFS-based algorithms, their multi-sensor generalization is computationally intractable [14]. As such, multi-sensor MTT remains an open problem

This paragraph of the first footnote will contain the date on which you submitted your paper for review.

S. Sruti and K. Giridhar are with the TelWiSe Group, Department of Electrical Engineering, Indian Institute of Technology, Madras, Chennai, India. (e-mail: srutisiva@telwise-research.com; k.giridhar@telwise-research.com)

from an implementation perspective.

Multi-target data association and localization for multistatic radar are achieved by various other techniques in literature. Empirical data association approaches also exist [15] [16]. The de-ghosting methods utilize all possible combinations of measurements and involve the calculation of metrics or geometric analyses in determining the correct associations. However, the complexity increases exponentially when the problem is scaled with many towers or targets, making implementation very difficult. The problem of de-ghosting is also solved using Bayesian analysis [17], or a Multi-Dimensional Assignment (MDA) scheme solved by S-D algorithm [18], or a group sparsity-based approach [19], etc. In all these approaches, which are challenging to implement in real-time, known distributions were used to model the birth and death processes of the targets and an initialization of the association to a specific state was also assumed. In [20], a "self-tuning" framework with belief propagation was proposed to adapt online to time-varying system models by continuously inferring unknown model parameters along with the target states. The complexity of this algorithm scaled only quadratically in the number of targets and linearly in the number of sensors, but accurate knowledge of the maximum number of targets was assumed in [20].

A. Tracking Filters

If the state and measurement models are linear and the probabilities are Gaussian, the Kalman Filter (KF) [21] is an efficient and optimal solution to the filtering problem in the least-squares sense. If the models are nonlinear, Unscented Kalman filter (UKF) [22], Extended Kalman Filter (EKF) [23] or Monte-Carlo methods [24] could be used. A PF [25] is used when linearizations and Gaussian approximations are intractable or yield an inadequate performance. When the targets are moving according to various kinematic models (maneuvering targets), in addition to associating measurements to targets and estimating their states, their models must also be evaluated at each point. Approximate methods such as Interacting Multi-Model (IMM) filters [10], where a bank of filters with each filter tuned to a specific model, is used to solve this problem. However, this is also computationally intensive.

Hence, to the best of our knowledge, there is no method currently available in open literature with a non-parametric and practically implementable approach for MTT-cum-data association for multistatic radar systems.

The motivation for our work is to design a real-time, computationally efficient data association and tracking algorithm for multiple targets in a multistatic radar system. The performance of this proposed *Non-Parametric Data Association and Tracking (NPDAT) algorithm* is compared to popular tracking algorithms to bring out the efficacy of our approach.

B. Notations and Paper Organization

The following notations are used in the paper. x, $\mathbf{x}$ and $\mathbf{X}$ represents scalar, vector and matrix respectively. diag($\mathbf{x}$) represents a diagonal matrix with $\mathbf{x}$ as the diagonal elements. $\mathbf{I_M}$ denotes a M-dimensional identity matrix.

The rest of the paper is organized as follows. The system model is illustrated in Section II. In Section III, the theory behind the system is explained and the problem of multiple target data association and tracking is formulated. The complete methodology of the NPDAT algorithm is described in Section IV. The algorithm is explained in Section V. Simulations to show the performance of the proposed algorithm in various scenarios and the comparison with existing algorithms is demonstrated in Section VI. Finally, the paper is summarized in Section VII.

II. System Model

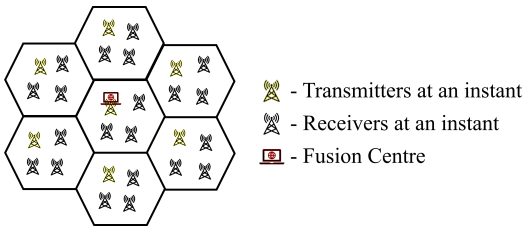

Fig. 1: Placement of Transmitters and Receivers at an Instant

The region of interest is a set of seven hexagonal cells with a 3 km inter-cell distance as shown in Fig. 1. Four static ground-based radar nodes acting as transmitters or receivers at an instant (referred to as towers) are randomly dropped in each cell. The height of the towers is taken randomly between 15 m and 25 m (comparable height). One of the towers in each cell acts as the transmitter and the others as receivers at any instant. This is referred to as a hop. Four such hops constitute one complete illumination cycle. The transmitters and receivers are time-synchronized, and the transmitters transmit orthogonal waveforms such that they are distinguishable at the receivers. Let N_t, N_r, and N_h denote the total number of transmitters, receivers, and hops, respectively. The measurements from the towers are sent to the fusion center, where they are further processed. A fixed fusion center at the center cell works independently for the set of seven cells. The NPDAT approach is implemented at this fixed fusion center. Thus, targets flying anywhere within the region of interest are correctly associated and tracked based on various separation levels. The targets outside the region of interest have fewer measurements and poor visibility as the fusion center is fixed. Hence, those targets are localized with comparatively higher error rates and thus are not continuously tracked correctly. This can be resolved by introducing appropriate interaction between the fusion centers, which, however, is beyond the scope of this current work.

III. Problem Formulation

Let $x_i[n]$ be the samples of the signal transmitted by the i^{th} transmitter. After getting reflected from the targets in the surveillance region, the discretized received signal at the j^{th} receiver is $y_j[n]$ and is given by,

$$y_j[n] = \sum_{i=1}^{N_t} \sum_{g=1}^{G} a_{i,j,g} x_i[n-\tau_{i,j,g}] exp(\frac{j2\pi f_{d_{i,j,g}} n}{f_s}) + w_j[n], \quad n = 0, ..., N-1 \quad (1)$$

This article has been accepted for publication in IEEE Journal of Selected Areas in Sensors. This is the author's version which has not been fully edited and content may change prior to final publication. Citation information: DOI 10.1109/JSAS.2024.3517513

where N_t and G denote the region's total number of transmitters and targets. Also, $a_{i,j,g}$, $\tau_{i,j,g}$ and $f_{d_{i,j,g}}$ are the complex amplitude indicating the propagation loss and RCS, Time-of-Arrival (TOA) and bistatic Doppler of the g^{th} target for the $(i,j)^{th}$ bistatic pair respectively. $w_j[n]$ represents i.i.d complex Gaussian noise with zero mean and variance σ^2.

At each receiver, $y_j[n]$ in (1) is sent through a bank of correlators with Doppler filters where it is cross-correlated with frequency-shifted replicas of the local copy of the transmit signal. This yields range-Doppler maps given by,

$$r_{y_{i,j}}[m,q] = \sum_{n=0}^{N-1} y_j[n]\bar{x}_i[n-m]exp(-j2\pi\frac{f'_{d_q}}{f_s}n), \quad m=0,...,N-1; q=0,...,Q-1 \tag{2}$$

where $r_{y_{i,j}}[m,q]$ denotes the correlated signal in the range-Doppler map with respect to $(i,j)^{th}$ bistatic pair and different Doppler hypothesis f'_{d_q}, f_s is the sampling frequency, $\bar{x}_i[n]$ represents the complex conjugate of the transmitted signal and Q denotes the total number of Doppler hypotheses. The correlated signal would have the highest peak in that Doppler bin, corresponding to the target's correct bistatic Doppler.

Targets are detected from (2) by a thresholding method. The threshold T_h is determined by estimating the approximate mean noise floor [26]. The TOA (also referred to as lag values) $\hat{\tau}_{i,j}$ and bistatic Doppler $\hat{f}_{d_{i,j}}$ measurements are obtained from the peaks in the range-Doppler map that have crossed T_h. The receivers record these measurements corresponding to each transmitter and forward them to the fusion center. At the fusion center, the measurements from each receiver are first associated with corresponding targets, and their positions and velocities are then estimated and tracked.

Note on the Impact of Constant False Alarm Rate (CFAR): Our model uses a high value of T_h, resulting in a low false alarm rate of 10^{-6}. However, false alarms can still occur. When the targets are far apart, the NPDAT algorithm clusters the TOA or the lag measurements from multiple bistatic pairs to different targets and localizes with only those measurements. The false alarms may mainly affect the NPDAT algorithm when the targets are close to each other. In this case, a hypothesis testing-based approach using the combinations method is used, which evaluates all possible measurement combinations across four bistatic pairs and selects those with the lowest ASOE (discussed in Section IV-B.5). This approach aims to mitigate the impact of false alarms by filtering out hypotheses with higher false alarm rates. Despite these measures, a minimal number of false alarms may persist, even in cases with lower ASOE. Operating at a low false alarm rate helps to minimize their occurrence, and the combinations method significantly reduces their impact. While complete elimination of false alarms may not be feasible, our approach substantially mitigates their effects.

IV. Methodology

A. Tracking

At time instant t=0 (initialization), all the estimated locations from the data association block are considered to belong to individual target tracks. The predicted position for the next time instant is determined depending on the position and velocity estimated in the current instant and is given by,

$$\hat{\mathbf{x}}_{k+1} = \hat{\mathbf{x}}_k + \hat{\mathbf{v}}_k t \tag{3}$$

From the next instant, if the lag estimates based on prediction fall within the validation region in the nearest neighbor sense uniquely, the corresponding lags are directly associated, localized, and then tracked. The lags corresponding to new-born or unassociated targets alone are then sent to the data association block. After localizing these targets, the targets are associated with the remaining tracks in the nearest neighbor sense or with new tracks. Tracks that are not updated for more than three instants are terminated.

B. Data Association

The algorithm follows a sequential approach and associates the measurements to targets at different separation levels. First, the targets are segregated based on various sub-levels of height differences as per Sections IV-B.1 and IV-B.2. If targets cannot be separated in these levels, then the second level of separation is performed for close-by targets as per Section IV-B.3.

1) Separation By Heights: The fusion center maintains the estimated lags with respect to the bistatic pairs in each hop in ascending order. Based on these lags, the maximum possible height within which the target would lie is determined based on the intersection of the coverage patterns of the transmitters and receivers in the region.

Creation of Maximum Height Dictionary: The surveillance region is divided into different height levels, $h \in 1,...,H$. For any height h, let the boundary of the surveillance region be represented by $(x_{\min}, x_{\max}, y_{\min}, y_{\max})$. This region is divided into a grid of bins based on a resolution res. Let $\mathbf{x} = (x,y,h)$ represent a bin in this hypothesised grid at this height h. The coverage of this bin from a given bistatic pair (i,j) is assured if the received Signal to Noise Ratio (SNR) along with the pulse compression gain (PC) during correlation is greater than the threshold (T_h), which is given by,

$$\frac{P_{r_{i,j}}}{N_p} + \text{PC} > T_h \tag{4}$$

where $\frac{P_{r_{i,j}}}{N_p}$ is the received SNR. The quantities in (4) are expressed in linear scale. N_p denotes the noise power and the received signal power $P_{r_{i,j}}$ is given by,

$$P_{r_{i,j}} = \frac{P_{t_i} G_{t_i} G_{r_j} \lambda^2 \sigma_{\min}}{(4\pi)^3 R_{t_i}^2 R_{r_j}^2} \tag{5}$$

where λ, G_{t_i}, G_{r_j}, R_{t_i} and R_{r_j} represent the wavelength of the signal, gain of i^{th} transmitter, gain of j^{th} receiver, and i^{th} transmitter-to-target and target-to-j^{th}receiver distances, respectively. These distances are inturn given by,

$$R_{t_i} = ||\mathbf{x} - \mathbf{x}_{t_i}|| \quad \text{and} \quad R_{r_j} = ||\mathbf{x} - \mathbf{x}_{r_j}|| \tag{6}$$

where $\mathbf{x}_t$ and $\mathbf{x}_r$ denote the transmitter and receiver coordinates respectively. Here, $\sigma_{\min}$ represents the minimum detectable target RCS based on the signal parameters taken

for simulation as mentioned in Table II. In the simulation considered, $\sigma_{\min} = 0.1$ m^2. The minimum detectable RCS can be lowered by correspondingly increasing the transmit power and the gains of the transmitting and receiving antennas. Hence, the NPDAT approach works irrespective of the target RCS. The lags corresponding to the grid of bins given by,

$$lag_{i,j} = \frac{(R_{t_i} + R_{r_j}) f_s}{c} \tag{7}$$

that satisfy the condition in (4) are alone retained in a set and the maximum of that set is taken as $\tau_{\text{dict}_{i,j,h}}$, where c in (7) denotes the speed of light. This is performed for all the bistatic pairs at different heights in the surveillance region and the maximum height dictionary is created. This initialization process is carried out only once during the placement of towers in the region. If new towers are added in the region, this process must be performed only for those towers. This procedure is summarized in Algorithm 1.

Fig. 2 depicts an example of the range of possible lag values for targets flying at different heights for a bistatic pair. As expressed in the figure, from a unique lag value of a target, it is impossible to decide the exact height of the target as the lag ranges will indeed overlap. However, the height within which the target will be flying can definitely be determined if the observation region is known.

Algorithm 1 Maximum Heights Dictionary

Input: $(x_{\min}, x_{\max}, y_{\min}, y_{\max})$

Output: $\tau_{\text{dict}_{i,j,h}} \forall i = 1, ..., N_t, j = 1, ..., N_r, h = 1, ..., H$

1: **for** i = 1 to N_t, j = 1 to N_r **do**
2: $\quad \mathbf{x}_{\text{iter}_{i,j,h}} = \emptyset$
3: $\quad \forall \mathbf{x} \in (x_{\min} : res : x_{\max}, y_{\min} : res : y_{\max}, h)$
4: $\quad$ **if** $\frac{G_{t_i} G_{r_j}}{R_{t_i}^2 R_{r_j}^2} \geq \frac{(T_h - \text{PC}) N_p (4\pi)^3}{\lambda^2 P_{t_i} \sigma_{\min}}$ **then**
5: $\quad\quad \mathbf{x}_{\text{iter}_{i,j,h}} = \mathbf{x}_{\text{iter}_{i,j,h}} \cup \mathbf{x}$
6: $\quad$ **end if**
7: $\quad \tau_{\text{dict}_{i,j,h}} = \frac{max(||\mathbf{x}_{\text{iter}_{i,j,h}} - \mathbf{x}_{t_i}|| + ||\mathbf{x}_{\text{iter}_{i,j,h}} - \mathbf{x}_{r_j}||) f_s}{c}$
8: **end for**
9: Repeat $\forall h = 1, .., H$
10: **return** τ_{dict}

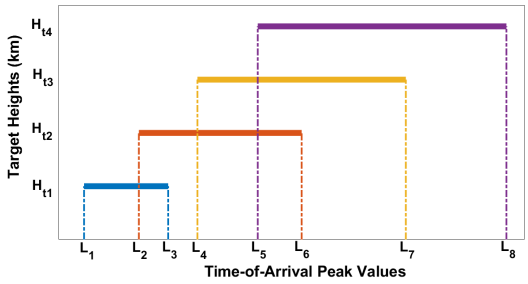

Fig. 2: Possible Lag Ranges for Targets at Different Heights

From the figure, it can be said that a target having a lag value of less than L_1 would surely be within H_{t1} height. Similarly, a target with a lag value of L_4 would surely be within H_{t3} height. However, a target with a lag value between L_2 and L_3 would be present anywhere between H_{t1} and H_{t2}, but it can be concluded that it would surely be within H_{t3} height. This inference is made only through the knowledge of the minimum lag value for targets at H_{t3} height. The maximum heights dictionary is constructed with this basic principle.

By mapping with the dictionary, the maximum possible height within which the target flies is determined for the lags in the lag table at the fusion center. Two targets are separable by heights for a bistatic pair if the range of maximum heights corresponding to the first set of lags does not overlap with the range of maximum heights corresponding to the second set of lags and so on. The target corresponding to l^{th} set of all lags in the table is separable if,

$$\begin{aligned} max(H_{m_{i,j,l-1}}) < min(H_{m_{i,j,l}}) \quad \text{and} \\ max(H_{m_{i,j,l}}) < min(H_{m_{i,j,l+1}}) \end{aligned} \tag{8}$$

where $H_{m_{i,j,l-1}}$ denotes the maximum height lookup entry for that lag set $l-1$ in the table for the $(i,j)^{th}$ bistatic pair.

If the targets are separable by heights in all the cells for all the hops, the corresponding lags can be directly associated and the targets can be localized individually. If the criterion of non-overlapping height ranges is satisfied only in one cell, the targets appear to be separated for that one cell. In that condition, the lag values corresponding to that cell are alone used for localization. However, this leads to an increase in the localization error as only fewer equations (a lesser number of lags) are used. To overcome this limitation, these estimated target locations are used as intermediate locations and the accurate locations are determined subsequently by an Ellipsoidal Ranging and Grouping (ERG) step as in IV-B.2. Based on the criterion of non-overlapping height ranges, the targets are classified into the following four categories:

TABLE I: Categories in Separation By Heights

Category	Description
(a)	In all the bistatic pairs of all the cells in all the hops
(b)	In all the bistatic pairs of all the cells in at least one hop
(c)	In the bistatic pairs of at least one cell in all the hops
(d)	In the bistatic pairs of at least one cell in at least one hop

Except for (a) and (b), if the given set of lags corresponds to the other categories, ERG is performed by which more lags are associated and the targets are localized accurately.

2) Ellipsoidal Ranging and Grouping (ERG): This technique is based on the concept of multi-lateration [27]. The input to this algorithm is the intermediate location along the x, y plane over which the target is present. A region around this intermediate location is considered and is divided into a grid of N_x x-bins and N_y y-bins. For each bin position (x, y), the feasible z estimate for the target is calculated from the lags corresponding to a chosen bistatic pair as follows:

$$d_{i,j} = \frac{lag_{i,j} \cdot c}{f_s} \tag{9}$$

Substituting (6) and (7) into (9) we get,

$$\hat{u} = \frac{-B \pm \sqrt{B^2 - 4AE}}{2A} \tag{10}$$

with,

$$A = (z_{t_i} - z_{r_j})^2 - B^2$$
$$B = V_3(z_{r_j} - z_{t_i}) + 2d_{i,j}^2 z_{r_j}$$
$$E = \frac{(V_3)^2}{4} - d_{i,j}^2 V_2 - d_{i,j}^2 z_{r_j}^2$$
$$V_1 = (x_{t_i} - x)^2 + (y_{t_i} - y)^2$$
$$V_2 = (x_{r_j} - x)^2 + (y_{r_j} - y)^2$$
$$V_3 = V_1 - V_2 + z_{t_i}^2 - z_{r_j}^2 - d_{i,j}^2$$

and the z estimate is then given by,

$$\hat{z} = max(\hat{u}) \tag{11}$$

Here, (11) evaluates the larger of the roots of the quadratic equation in an efficient one-line equation and can be calculated in parallel for all the bins.

If $\hat{z}$ falls within the possible z range (given by the maximum heights permissible in the dictionary), the corresponding $(x, y, \hat{z})$ coordinates is regarded as a candidate position for the target. The minimum and maximum lags possible for all the bistatic pairs are found with these candidate positions. Based on the determined ranges of lags and recorded lag values in all the bistatic pairs, the lags are grouped to the targets accordingly and targets are localized with these associated lags. This step is done only if unique lags fall into non-overlapping ranges and is summarized in Algorithm 2.

The efficiency of this method depends on the resolution of bin sizes and the size of the intermediate region. The smaller the intermediate region and bin size, the more accurate the estimated target positions are, as a result of more lags getting grouped. A trade-off exists between the computational time and the number of bins considered in the intermediate region.

Algorithm 2 Ellipsoidal Ranging and Grouping

Input: $lag_{i,j}$ and intermediate location $(\hat{x}, \hat{y})$ of target
Output: More grouped lags based on $L_{\max_{i,j}}$ and $L_{\min_{i,j}}$

for i = 1 to N_t, j = 1 to N_r **do**
  $\mathbf{x}_{\text{iter}_{i,j}} = \emptyset$, $\hat{\mathbf{lag}}_{i,j} = \emptyset$
  Intermediate region around $(\hat{x}, \hat{y})$ is divided into N_x x bins and N_y y bins
  for a = 1 to N_x, b = 1 to N_y **do**
    $\forall$ bin position (x, y)
    if $\hat{z} \leq H_{m_{i,j}}$ **then**
      $\mathbf{x} = (x, y, \hat{z})$
      $\mathbf{x}_{\text{iter}_{i,j}} = \mathbf{x}_{\text{iter}_{i,j}} \cup \mathbf{x}$
      Calculate lag value τ for $\mathbf{x}$ as per (7)
      $\hat{\mathbf{lag}}_{i,j} = \hat{\mathbf{lag}}_{i,j} \cup \tau$
    end if
  end for
  $L_{\max_{i,j}} = max(\hat{\mathbf{lag}}_{i,j})$, $L_{\min_{i,j}} = min(\hat{\mathbf{lag}}_{i,j})$
end for
Group recorded lags $lag_{i,j}$ based on estimated $L_{\max_{i,j}}$ and $L_{\min_{i,j}}$
return Associated lags

3) Combinations Method for Close-By Targets: This is the separation level used for the data association of close-by targets. This method necessitates finding at least four lags corresponding to targets close by to estimate the intermediate position. One transmitter and four receivers are chosen and with the lags corresponding to these bistatic pairs, different combinations of lags are generated [15]. For each of these, target positions are estimated and only those with ASOE $< T_0$ (as discussed in Section IV-B.5) are identified as correct target position estimates. However, this results in low estimation accuracy as only four unique equations are involved in the localization process. Therefore, the estimates are considered as intermediate locations and processed further using ERG.

When one transmitter and four receivers are chosen (four bistatic pairs), if there are G targets in the surveillance region, the maximum number of possible lag combinations would be G^4. The complexity of this method increases exponentially as the number of targets increases. However, the complexity is capped since only one transmitter and four receivers are selected for this method. The number of possible combinations is also minimized by using ERG. The time complexity can be combated by performing the localization corresponding to different combinations of lags in parallel as it only involves computation of 3×3 inverses [28]. Since this technique is used only for close-by targets, the implementation complexity of the algorithm is still limited and thus practically implementable. The set of one transmitter and four receivers whose lag values are used for generating the combinations of lags is chosen by using one of the following two approaches:

- Approach A - Inclusive Periphery Algorithm (IPA):
  The transmitter with maximum number of lags with respect to the receivers is selected. Receivers are chosen from all four quadrants in such a way that they are present at the farthest distance from the selected transmitter.
- Approach B - Tight Periphery Algorithm (TPA):
  If the receivers on all four quadrants could not be chosen as per Approach A, then they are selected as follows: Three receivers are chosen from the same cell as the selected transmitter and the fourth receiver is chosen from any other cell such that it has the least distance from the selected transmitter.

The idea behind both of these approaches is to maximize horizontal diversity for better localization. If such transmitters and receivers are not present as per Approach A, then the towers are chosen so the target is enclosed within their locations.

4) Localization and Velocity Estimation: Once the lags are associated with the targets, it is localized by following closely the algorithm in [28]. The locus of the points corresponding to the distance derived from the TOA value is an ellipsoid with the corresponding transmitter and receiver at its foci. The intersection of the ellipsoids determines the position of the target. Due to the lower height diversity in ground-based towers, the accuracy of height estimates suffers. Hence, after obtaining the position estimates, the height estimate is further improved using the modified least squares framework. Using estimated $d_{i,j}$ in (9), the following set of bistatic equations are formulated:

$$\mathbf{S}_i\mathbf{x} = \mathbf{z}_i + \mathbf{r}_i R_{t_i} \tag{12}$$

$$R_{t_i} = ||\mathbf{x}_{t_i} - \mathbf{x}||$$
$$\mathbf{S}_i = \begin{pmatrix} \mathbf{x}_{r_1}^T - \mathbf{x}_{t_i}^T \\ . \\ . \\ \mathbf{x}_{r_{N_r}}^T - \mathbf{x}_{t_i}^T \end{pmatrix} \quad \mathbf{r}_i = \begin{pmatrix} d_{i,1} \\ . \\ . \\ d_{i,N_r} \end{pmatrix} \tag{13}$$
$$\mathbf{z}_i = \frac{1}{2} \begin{pmatrix} ||\mathbf{x}_{r_1}||^2 - d_{i,1}^2 - ||\mathbf{x}_{t_i}||^2 \\ . \\ . \\ ||\mathbf{x}_{r_{N_r}}||^2 - d_{i,N_r}^2 - ||\mathbf{x}_{t_i}||^2 \end{pmatrix}$$

The nuisance parameter R_{t_i} is removed by pre-multiplying (12) by $\mathbf{M}_i = \mathbf{V}^T\mathbf{D}_i$ where $\mathbf{D}_i = ((diag(\mathbf{r}_i))^{-1}$. Here, $\mathbf{V}$ is obtained from the SVD of $[\mathbf{I}_{N_r} - \mathbf{Z}]$ where $\mathbf{Z}$ is a circular shift matrix [28]. Thus,

$$\mathbf{M}_i\mathbf{S}_i\mathbf{x} = \mathbf{M}_i\mathbf{z}_i \tag{14}$$

All such equations for the N_t transmitters over one cycle of hops are stacked and are expressed in matrix form as,

$$\mathbf{A}\mathbf{x} = \mathbf{b} \tag{15}$$

Due to the measurement errors and noise in the bistatic range estimation, only noisy versions of $\mathbf{A}$ and $\mathbf{b}$, $\hat{\mathbf{A}}$ and $\hat{\mathbf{b}}$ are obtained. Hence, the position estimate is given by,

$$\hat{\mathbf{x}} = (\hat{\mathbf{A}}^T\hat{\mathbf{A}})^{-1}\hat{\mathbf{A}}\hat{\mathbf{b}} \tag{16}$$

With the position estimates of targets obtained in localization and the corresponding associated bistatic Doppler measurements, the velocities of the targets are estimated following [15]. Due to the measurement errors and noise in bistatic Doppler estimation, noisy versions $\hat{\mathbf{Y}}$ and $\hat{\mathbf{z}}$ are used instead of $\mathbf{Y}$ and $\mathbf{z}$, which is written as,

$$\hat{\mathbf{v}} = (\hat{\mathbf{Y}}^T\hat{\mathbf{Y}})^{-1}\hat{\mathbf{Y}}\hat{\mathbf{z}} \tag{17}$$

where,

$$\mathbf{Y} = \begin{pmatrix} \frac{x-x_{r_1}}{R_{r_1}} + \frac{x-x_{t_1}}{R_{t_1}} & \frac{y-y_{r_1}}{R_{r_1}} + \frac{y-y_{t_1}}{R_{t_1}} & \frac{z-z_{r_1}}{R_{r_1}} + \frac{z-z_{t_1}}{R_{t_1}} \\ . & . & . \\ \frac{x-x_{r_{N_r}}}{R_{r_{N_r}}} + \frac{x-x_{t_1}}{R_{t_1}} & \frac{y-y_{r_{N_r}}}{R_{r_{N_r}}} + \frac{y-y_{t_1}}{R_{t_1}} & \frac{z-z_{r_{N_r}}}{R_{r_{N_r}}} + \frac{z-z_{t_1}}{R_{t_1}} \\ . & . & . \\ \frac{x-x_{r_1}}{R_{r_1}} + \frac{x-x_{t_{N_t}}}{R_{t_{N_t}}} & \frac{y-y_{r_1}}{R_{r_1}} + \frac{y-y_{t_{N_t}}}{R_{t_{N_t}}} & \frac{z-z_{r_1}}{R_{r_1}} + \frac{z-z_{t_{N_t}}}{R_{t_{N_t}}} \\ . & . & . \\ \frac{x-x_{r_{N_r}}}{R_{r_{N_r}}} + \frac{x-x_{t_{N_t}}}{R_{t_{N_t}}} & \frac{y-y_{r_{N_r}}}{R_{r_{N_r}}} + \frac{y-y_{t_{N_t}}}{R_{t_{N_t}}} & \frac{z-z_{r_{N_r}}}{R_{r_{N_r}}} + \frac{z-z_{t_{N_t}}}{R_{t_{N_t}}} \end{pmatrix}$$

$$\mathbf{z} = \begin{pmatrix} d'_{1,1} \\ . \\ d'_{N_r,1} \\ . \\ d'_{1,N_t} \\ . \\ d'_{N_r,N_t} \end{pmatrix} \tag{18}$$

and, $d'_{j,i}$ is the bistatic range rate with respect to $(i,j)^{th}$ bistatic pair, and is expressed as

$$d'_{j,i} = \frac{d}{dt}(R_{t_i} + R_{r_j}) = -f_{d_{i,j}}\lambda \tag{19}$$

After localizing each target, the corresponding unassociated lags from other bistatic pairs are eliminated so that they do not interfere with the association of other targets.

5) Absolute Sum of Errors (ASOE): It is a metric defined to check for the correctness of the localization estimate. Similar to the Weighted Sum of Squares (WSOS) in [15], it checks for consistency between the actually measured bistatic ranges and the estimated bistatic ranges from the position estimates. Let $d_{c,i,j}$ and $\hat{d}_{c,i,j}$ be the measured and estimated bistatic ranges corresponding to hop c, transmitter i and receiver j respectively. The ASOE is given by:

$$\text{ASOE} = \sum_{c=1}^{N_h}\sum_{i=1}^{N_t}\sum_{j=1}^{N_r}|d_{c,i,j} - \hat{d}_{c,i,j}| \tag{20}$$

If ASOE $<$ Threshold (T_0) (appropriately chosen as discussed in [27]), the position estimate corresponds to a true target. A higher ASOE value implies a higher error in localization.

V. NPDAT Algorithm Flow

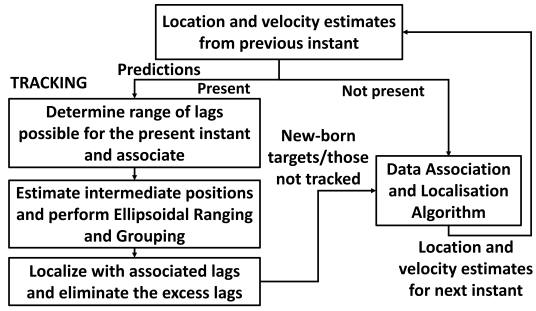

Fig. 3: Outline of the NPDAT Algorithm

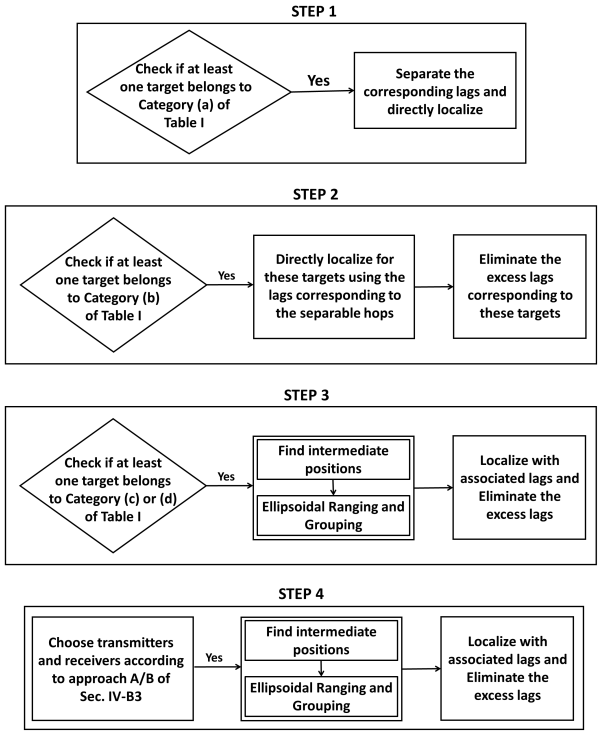

Fig. 4: The Four Steps in the Data Association Section

The complete flow of the NPDAT algorithm is illustrated in Fig. 3. The algorithm quickly tracks those targets whose positions and velocities of targets in the previous instants are

available, if the measured lags fall within the validation region of the estimated lags with respect to the different bistatic pairs. The data association algorithm is performed only for newborn and non-trackable targets at the current instant.

The data association section of the NPDAT algorithm is broken down into the following four steps as shown in Fig. 4. Step 1: Sort out targets separated by heights belonging to category (a) as specified in Table I and directly localize them. Step 2: Segregate targets separated by heights belonging to category (b) as specified in Table I and directly localize them. Step 3: Segregate targets separated by heights belonging to category (c) or (d) as specified in Table I. Associate maximum number of lags through ERG and localize the targets.
Step 4: This step utilizes the method discussed in Section IV-B.3 to identify and localize closely spaced targets. Step 4 can be broken down into two parts: (4A) and (4B). Here, (4A) and (4B) involve choosing the transmitters and receivers according to approaches A and B of Section IV-B.3, respectively. Intermediate locations are found, ERG associates a maximum possible number of lags, and the targets are localized.
Flow of the data association algorithm is outlined in Fig. 5.

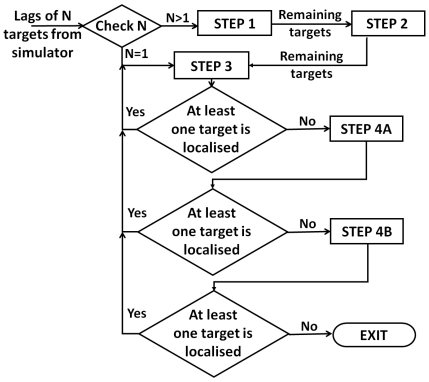

Fig. 5: Outline of Data Association Section

VI. Simulation Results

The algorithm is tested in a simulation environment developed in Matlab. It simulates a multistatic radar setup with distributed transmitters and receivers with the following system parameters as given in Table II. The coverage of the transmitters and receivers is bounded primarily because of their antenna patterns. Thus, all the targets cannot be observed in all the bistatic pairs. The algorithm is tested with such a varying number of misdetections in various bistatic pairs. Based on the link budget of the system, the detection of targets with a minimum RCS σ_{min} is assured for the entire surveillance region. The RCS of the targets is taken anywhere between 0.1 m^2 to 1.0 m^2 in the simulation. The threshold (T_h) is set such that the false alarm rate is 10^{-6} with respect to the lowest possible RCS (σ_{min}= 0.1 m^2). The TOA and bistatic Doppler measurements of targets corresponding to the bistatic pairs are determined as explained earlier in Section III.

A. Association - Multiple Targets Appearing "All at Once"

The algorithm has been tested by simulating 2, 3, and 4 targets appearing at once in the surveillance region. Initialization is not needed for the process. The targets are assumed to move with arbitrary velocities ranging from 50 m/s to 150 m/s. Different scenarios have been considered with targets at different height differences and varying x-y separations. As a result of the antenna patterns of the transmitters and receivers, all the bistatic pairs cannot observe all the targets, and not all bistatic pairs report the same number of lag values. It is worth mentioning that the algorithm has been developed to adapt to such situations without knowing or explicitly estimating the number of targets. Height differences between the targets vary from 3 km to targets flying at the same height. The x, y separation between the targets varies from 1 km to 100 m. In each combination of this separation, 300 Monte Carlo (MC) simulations have been performed with independently generated measurements, and the consolidated results, rounded to the nearest meter, are alone presented in Tables III and IV. 3D position and velocity estimation accuracies are measured by Root Mean Square Error (RMSE) in each coordinate, which is given by,

TABLE II: Simulation Parameters

Parameters	**Values**
Inter-Cell Distance	3 km
Bandwidth (B)	20 MHz
Number of Targets (G)	2,3 or 4
Antenna Gain	18 dBi
Number of Towers in the Region	28 (4 towers in each cell)
Doppler Bin Resolution	100 Hz
Transmit Power (P_t)	100 W

$$\text{PosRMSE}_k = \sqrt{\frac{1}{M_c}\sum_{m=1}^{M_c}(|\mathbf{x}_k - \hat{\mathbf{x}}_k|^2)} \tag{21}$$

$$\text{VelRMSE}_k = \sqrt{\frac{1}{M_c}\sum_{m=1}^{M_c}(|\mathbf{v}_k - \hat{\mathbf{v}}_k|^2)} \tag{22}$$

where $\mathbf{x}_k$ and $\mathbf{v}_k$ denote the true position and velocity coordinates, $\hat{\mathbf{x}}_k$ and $\hat{\mathbf{v}}_k$ denote the estimated position and velocity coordinates of the k^{th} target respectively and M_c denote the total number of MC runs.

Table III shows the 3D position accuracy for this scenario. As per the results, the position RMSE (PosRMSE) indicates high precision in location estimation. There is an increase in error for certain cases (shown as the maximum error which is denoted by Max. Error). This occurs when targets are present at the corners of the outer cells, resulting in fewer bistatic pairs seeing the targets. Thus, for these targets, there is a lower accuracy in localization, which can be combated by introducing interaction between adjacent fusion centers. When three and four targets are present at once at the same height within 100 m $\times$ 100 m ambiguity region (region within which if the targets are present, the estimation accuracy drops), error shoots up higher than the mean for 1.4% and 2.8% of the trials respectively. As more targets are present closely, the localization accuracy decreases, or the ambiguity region increases. This is because, during the initial phase of the algorithm, lags of all the targets seen from all the bistatic pairs are taken together for the association process. Hence, there is greater interference from other targets. This ambiguity region depends on the bandwidth considered. The bandwidth used

for the signals is only 20 MHz. If the bandwidth is increased, the bistatic range resolution improves. Hence, the ambiguity region decreases, and localization accuracy improves.

TABLE III: Position Localization Accuracy

G	Separation between targets	PosRMSE $[\mathbf{x}, \mathbf{y}, \mathbf{z}]$ (m)	Max. Error $[\mathbf{x}, \mathbf{y}, \mathbf{z}]$ (m)
2	Any height difference and $\geq$ 100 m in either x or y	[2,1,2]	[6,5,12]
3	500 m and above height difference and $\geq$ 100 m in either x or y	[2,2,2]	[9,7,12]
	Same height and $\geq$ 200 m in either x or y	[1,1,2]	[5,4,11]
	Same height and 100 m in either x or y	[3,3,5]	[33,48,63]
4	500 m and above height difference and $\geq$ 100 m in either x or y	[2,1,2]	[10,10,11]
	Same height and $\geq$ 200 m in either x or y	[1,1,2]	[4,4,12]
	Same height and 100 m in either x or y	[2,3,5]	[22,27,56]

TABLE IV: Velocity Estimation Accuracy

G	Separation between targets	VelRMSE $[\mathbf{v_x}, \mathbf{v_y}, \mathbf{v_z}]$ (m/s)	Max. Error $[\mathbf{v_x}, \mathbf{v_y}, \mathbf{v_z}]$ (m/s)
2	Any height difference and $\geq$ 100 m in either x or y	[2,2,3]	[8,7,20]
3	Any height difference and $\geq$ 100 m in either x or y	[2,3,3]	[10,7,19]
4	Any height difference and $\geq$ 100 m in either x or y	[3,3,4]	[10,8,22]

In the algorithm, the step with the highest computational complexity is Step 4 of Section V. For all target cases (2,3,4), only the trials corresponding to targets flying at a height difference of 500 m or less with $x-y$ separation less than or equal to 500 m reach this step. Of these, only about 3 to 5% of them tend to go to approach B of Section IV-B.3. Thus, approach B improves accuracy, albeit at a slightly higher computational cost. The velocity estimation results are presented in Table IV. Based on the lags associated with targets, bistatic Doppler measurements are taken for velocity estimation. The accuracy thus depends upon the extent of grouping of lags to the targets. Since the Doppler bin resolution in the simulator is 100 Hz, the maximum velocity error goes up to [10,8,22] m/s. If the Doppler bin resolution is improved, the maximum error in velocity estimation will be reduced.

B. Association and Tracking

The performance of the NPDAT algorithm with sequential occurrence and random death of the targets at different positions with arbitrary velocities in all three coordinates from 50 m/s to 150 m/s are shown. Each instant, also called the update rate $t_{\max}$, is the time the following data set is processed. One target appears at every instant, moving in any random direction. The algorithm is tested with $t_{\max}$=100 ms. The RMSE and maximum error values for position and velocity estimation for the targets at different instants are presented in Table V and Table VI respectively.

A spike in error seen in the last row of Table V during the later instants is due to reduced separation or cross-over between the targets. Except in the first instant, in the presence of previous track updates, the algorithm rarely goes to Step 4. With the inclusion of tracking, the number of trials entering Step 4 reduces by 25%. Also, as per results in Table VI, it can be observed that the accuracy of velocity estimation has also improved in comparison with Table IV.

TABLE V: Localization Accuracy - Sequential Birth

$\mathbf{t_{max}}$	Separation between targets	Instants	PosRMSE $[\mathbf{x}, \mathbf{y}, \mathbf{z}]$ (m)	Max. Error $[\mathbf{x}, \mathbf{y}, \mathbf{z}]$ (m)
100 ms	500 m and above height difference and $\geq$ 100 m in either x or y	All	[3,3,3]	[8,12,15]
	Same height and 500 m in either x or y	All	[2,2,3]	[6,7,13]
	Same height and 200 m in both x and y	All	[2,2,3]	[6,5,17]
	Same height and 200 m either along only x or only y	Till 8th	[2,2,4]	[6,6,16]
		Only at 9th	[2,2,6]	[35,60,37]

TABLE VI: Velocity Estimation Accuracy - Sequential Birth

$\mathbf{t_{max}}$	Separation between targets	Instants	VelRMSE $[\mathbf{v_x}, \mathbf{v_y}, \mathbf{v_z}]$ (m/s)	Max. Error $[\mathbf{v_x}, \mathbf{v_y}, \mathbf{v_z}]$ (m/s)
100 ms	500 m and above height difference and $\geq$ 100 m in either x or y	All	[3,3,4]	[10,8,14]
	Same height and $\geq$ 200 m in either x or y	All	[2,2,4]	[8,7,14]

C. Comparison with Existing Algorithms

The assignment-based multi-target tracking algorithms compared with the NPDAT algorithm are GNN, JPDA, and MHT [12]. GNN and JPDA are single-scan methods, whereas MHT is a multi-scan method. The measurement model is non-linear, so the tracking filter used is EKF. Using the Jacobian matrix in the KF equations essentially linearizes the function around the current estimate. The assignment for tracking is done using the S-D assignment solved using the Lagrangian relaxation method [3].

Constant Velocity (CV), Constant Acceleration (CA), and Constant Turn (CT) are the state models used for tracking depending upon the scenario considered. However, more than one model is essential to track targets with motion uncertainty. Hence, IMM is used where it assumes a set of models as possible candidates of the true mode each time and runs a bank of elemental filters, each based on a unique model in the set. The overall estimate is generated based on the results of these elemental filters. Each estimated target is assigned to at least one track. A new track is created if it cannot be assigned to any existing track. Any new track is started in a tentative state. If enough assignments are done to the tentative track (at least two in the last three updates), its status is changed to confirmed. If enough assignments are not done to the confirmed track within a specific number of updates (three in the last three updates),

This article has been accepted for publication in IEEE Journal of Selected Areas in Sensors. This is the author's version which has not been fully edited and content may change prior to final publication. Citation information: DOI 10.1109/JSAS.2024.3517513

the track is deleted. For MHT implementation, the maximum number of track branches allowed for each track is three, and the maximum number of global assignment hypotheses maintained at each step is fixed as five.

The performance metric used for the comparison of the algorithms is the RMSE of the position and velocity estimates of the targets given by,

$$\text{RMSE} = \sqrt{\frac{1}{N_{\text{inst}} N_{\text{coord}}} \sum_{n=1}^{N_{\text{inst}}} (||\mathbf{x} - \hat{\mathbf{x}}||^2)} \tag{23}$$

where $\mathbf{x}$ and $\hat{\mathbf{x}}$ denote the true and estimated position or velocity vectors of targets, N_{inst} and N_{coord} denote the total number of time instants the targets' movements are recorded and the total number of coordinates (x, y, z) which is equal to 3 respectively.

1) Difference between Existing Association-cum-Tracking Approaches and NPDAT: The contrast between the basic approach of NPDAT and the other algorithms is highlighted in the table.

Existing Algorithms	NPDAT Algorithm
Considers **all the possible associations** from multiple bistatic pairs, localises, retains those with least cost and assigns to tracks based on specific methods	**Clusters TOA values** from multiple bistatic pairs to different targets, localises only those and assigns to tracks based on predictions of nearest neighbours
Estimated positions may have **correct targets as well as false alarms/random clutter**	Estimated positions have **only the correct targets** as the TOA values are clustered to targets and only those are localized. Hence, TOA values of false alarms may not be grouped to any targets as they will be random
Highly **parametric** on number of targets and motion models	**Non-parametric** and hence no assumption on the number of targets and motion models
Localises targets even within ambiguity region but **does not associate** them to tracks correctly	**Does not localise as well as track** targets within ambiguity region

2) Ability to Handle Maneuvering Targets: A combination of CV, CA, and CT models is used to incorporate the targets' motion maneuverability. The extent of change in motion is brought by varying parameters like linear velocity, acceleration, and angular velocity. Fig. 6 shows the true trajectory of two targets maneuvering slow and fast. The tracking ability of the various algorithms when the targets are maneuvering slowly is shown in Fig. 7. GNN-IMM creates many tracks as it cannot handle frequent motion changes. JPDA-IMM, MHT-IMM, and NPDAT track the targets precisely. The analysis in terms of RMSE in position and velocity estimation for both the targets is shown in Table VII. The error performance for the above three algorithms is also approximately the same.

TABLE VII: Estimation Accuracy - Slow Maneuvering Targets

RMSE	GNN-IMM	JPDA-IMM	MHT-IMM	NPDAT
Position (m)	3.15 3.43	2.08 2.68	1.90 2.43	1.83 1.56
Velocity (m/s)	29.02 20.15	3.63 5.68	3.01 3.28	2.72 3.52

The tracking ability of the algorithms for fast maneuvering

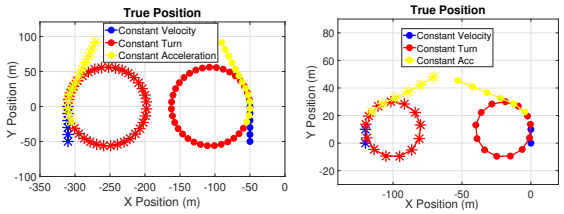

Fig. 6: True Trajectory - a) Slow b) Fast Maneuvering Targets

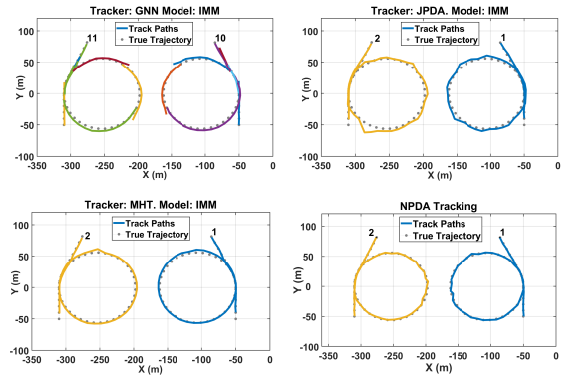

Fig. 7: Tracking Ability of Algorithms - Slow Maneuver

targets is captured in Fig. 8. NPDAT precisely tracks the fast change in the target's motion. GNN-IMM, JPDA-IMM, and MHT-IMM exhibit poor tracking performance as the extent of maneuverability here is very rapid. The estimation performance analysis in terms of RMSE in position and velocity for both the targets is shown in Table VIII. In addition to rightly tracking the targets, NPDAT is shown to have the least error in estimating position and velocity.

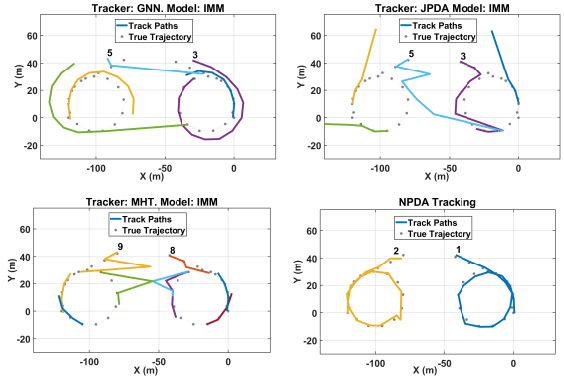

Fig. 8: Tracking Ability of Algorithms - Fast Maneuver

TABLE VIII: Estimation Accuracy - Fast Maneuvering Targets

RMSE	GNN-IMM	JPDA-IMM	MHT-IMM	NPDAT
Position (m)	56.47 23.91	37.30 26.85	9.01 12.99	1.03 1.67
Velocity (m/s)	106.91 87.71	46.30 84.04	44.32 89.82	3.55 3.96

3) Ability to Handle Close-By Targets: The ability to track the close-by targets is analyzed by simulating two targets whose true trajectory is shown in Fig. 9. The least distance between the two targets is 40 m. For successful association and tracking by the NPDAT algorithm, two targets should be

separated by ± 1 lag, which approximately comes to 40 m in close $x-y$ or height separation. The tracking ability of the algorithms is illustrated in Fig. 10. MHT-IMM tracks better than GNN-IMM and JPDA-IMM. However, when the targets are undergoing the turn motion, all the above three algorithms fail to get them onto their tracks. NPDAT tracks the targets irrespective of their change in motion. The only criterion for NPDAT to track targets is that their least distance should be greater than that corresponding to ± 1 lag. The performance in Table IX indicates that NPDAT has good estimation accuracy in addition to correct target tracking.

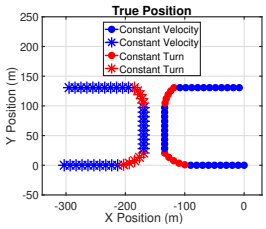

Fig. 9: True Trajectory - Close-By Targets

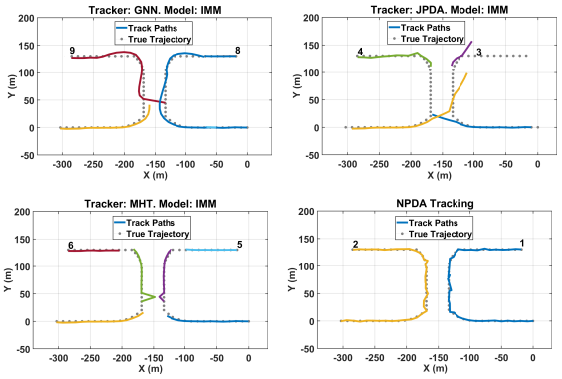

Fig. 10: Tracking Ability of Algorithms - Close-By Targets

TABLE IX: Estimation Accuracy - Close-By Targets

RMSE	GNN-IMM	JPDA-IMM	MHT-IMM	NPDAT
Position (m)	60.98 5.24	14.59 20.58	1.83 3.87	1.98 1.79
Velocity (m/s)	59.00 39.63	47.50 31.95	8.15 21.99	5.21 5.84

4) Ability to Handle Cross-Over Targets: Two targets fly at a height difference of 40 m whose true trajectories are plotted in Fig. 11. In the first scenario, the targets cross each other and proceed with the same velocity. In the second scenario, the targets come face-to-face and go back with an abrupt change in velocity. The tracking results for the cross-over scenario are shown in Fig. 12, and the performance for both the targets is demonstrated in Table X. CV model is used for the tracking filters for this analysis. All the algorithms track the targets properly. NPDAT has slightly greater RMSE than the conventional algorithms. This is because, in conventional approaches, all the possible combinations of lags from all the bistatic pairs are utilized to obtain target positions. However, in NPDAT, only the clustered lags from various bistatic pairs corresponding to different targets are used for the same.

The tracking results for the meet-go-back scenario is captured in Fig. 13 and error metrics for the same is shown in

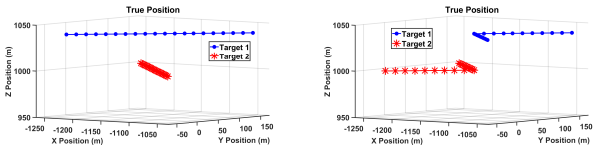

Fig. 11: True Trajectory - a) Cross-Over b) Meet-Go-Back

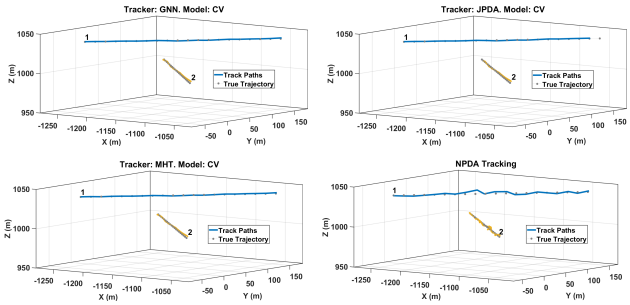

Fig. 12: Tracking Ability of Algorithms - Cross-Over

TABLE X: Estimation Accuracy - Cross-Over Targets

RMSE	GNN-CV	JPDA-CV	MHT-CV	NPDAT
Position (m)	1.27 1.68	1.17 1.65	1.26 1.68	1.69 1.81
Velocity (m/s)	5.12 6.38	4.04 6.57	5.08 4.23	5.06 5.72

Table XI. The existing algorithms fail to track the targets in this case. Even the IMM model for these algorithms did not exhibit good tracking performance. Observe that only NPDAT tracks the targets correctly.

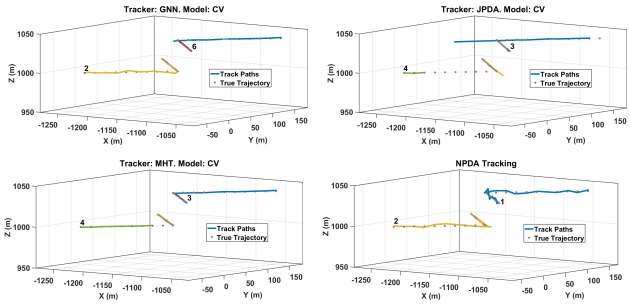

Fig. 13: Tracking Ability of Algorithms - Meet-Go-Back

TABLE XI: Estimation Accuracy - Meet-Go-Back Targets

RMSE	GNN-CV	JPDA-CV	MHT-CV	NPDAT
Position (m)	4.65 5.38	27.39 26.97	1.24 0.99	2.16 1.79
Velocity (m/s)	30.02 29.09	36.87 38.23	21.31 21.38	9.42 15.55

5) Time Complexity: The average time taken for data association and tracking is determined for all the algorithms, with two and four targets moving in arbitrary directions. The time taken is measured as the run-time of the algorithms' Matlab implementation. The processor used was an Intel i7-6700 clocked at 3.4 GHz utilizing 16 GB of DDR4 2133 MHz RAM. The total number of possible measurement associations for the assignment-based approaches is $(G)^{N_t \times N_r}$ where G, N_t and N_r are the number of targets, transmitters and receivers respectively in the region. Since there is a greater number of

transmitters and receivers, the number of possible associations for these approaches is reduced by gating. The time taken per instant for a two-target scenario is shown in Fig. 14. The data association assignment part for the other algorithms consumes most of the run-time (103.76 s). It is observed that the run-time for NPDAT is almost 100 times less than the existing algorithms.

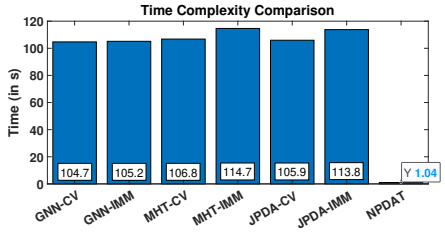

Fig. 14: Average Time Taken per Instant - Two Targets

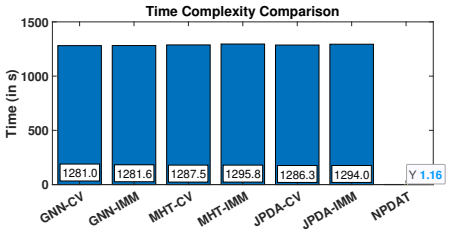

Fig. 15: Average Time Taken per Instant - Four Targets

The time taken per instant for a four-target scenario is shown in Fig. 15. The run-time increases exponentially for the assignment-based tracking approaches. The time taken for the data association part is 1278.58 s. The increase in the number of targets in the scenario has increased the run-time for NPDAT only in the order of milliseconds. This shows the time efficiency and, hence, the scope of real-time implementation possibility of the NPDAT algorithm compared to the other algorithms.

6) Note on Algorithm Complexity: The existing algorithms take into account all the possible measurement associations. Localization and cost calculation are performed for all these associations. This is the costliest step as the complexity increases exponentially as the number of targets, transmitters, or receivers increases. The IMM-based approaches reasonably estimate the target's mode if the targets are maneuvering. However, its implementation adds to the complexity. These reasons question the chance of real-time execution of these approaches. NPDAT follows a sequential approach but never requires processing all the associations. Even in the association of closeby targets, it considers associations only from four bistatic pairs. Hence, the computational complexity of NPDAT is minimal.

VII. Conclusion

A novel and efficient sequential data association and tracking algorithm has been developed based on the underlying geometrical aspects of a multistatic radar system. This Non-Parametric Data Association and Tracking (NPDAT) approach does not require knowledge of the number of targets or their motion models. It does not assume any initial state for the targets and works with more than one target appearing simultaneously in the surveillance region. The performance of the data association and tracking algorithm for targets flying with arbitrary velocities at various heights and horizontal separation levels was presented. The ambiguity region and cap on accuracy for a given number of targets are dependent on the implementation parameters, such as signal bandwidth, Doppler resolution, and the speed of the targets desired to be detected. NPDAT displayed enhanced tracking performance even with significantly lower run-time and algorithm complexity compared to the existing algorithms. The proposed NPDAT approach is, therefore, amenable for practical implementations.

References

[1] A. M. Haimovich, R. S. Blum, and L. J. Cimini, "MIMO Radar with Widely Separated Antennas," *IEEE Signal Processing Magazine*, vol. 25, no. 1, pp. 116–129, 2008.

[2] T. Fortmann, Y. Bar-Shalom, and M. Scheffe, "Sonar Tracking of Multiple Targets using Joint Probabilistic Data Association," *IEEE Journal of Oceanic Engineering*, vol. 8, no. 3, pp. 173–184, 1983.

[3] S. Deb, M. Yeddanapudi, K. Pattipati, and Y. Bar-Shalom, "A Generalized S-D Assignment Algorithm for Multisensor-Multitarget State Estimation," *IEEE Transactions on Aerospace and Electronic Systems*, vol. 33, no. 2, pp. 523–538, 1997.

[4] M. Tobias and A. Lanterman, "Probability Hypothesis Density-Based Multitarget Tracking with Bistatic Range and Doppler Observations," *IEE Proc. Radar, Sonar and Navigation*, vol. 152, no. 3, p. 195, 2005.

[5] E. Kamen, "Multiple Target Tracking Based on Symmetric Measurement Equations," *IEEE Transactions on Automatic Control*, vol. 37, no. 3, pp. 371–374, 1992.

[6] S. Blackman, "Multiple Hypothesis Tracking for Multiple Target Tracking," *IEEE Aerospace and Electronic Systems Magazine*, vol. 19, no. 1, pp. 5–18, 2004.

[7] C. Hue, J.-P. Le Cadre, and P. Perez, "Tracking Multiple Objects with Particle Filtering," *IEEE Transactions on Aerospace and Electronic Systems*, vol. 38, no. 3, pp. 791–812, 2002.

[8] Y. Bar-Shalom, F. Daum, and J. Huang, "The Probabilistic Data Association Filter," *IEEE Control Systems Magazine*, vol. 29, no. 6, pp. 82–100, 2009.

[9] Y. Bar-Shalom and X. Li, *Multitarget-Multisensor Tracking: Principles and Techniques*. Yaakov Bar-Shalom, 1995.

[10] E. Mazor, A. Averbuch, Y. Bar-Shalom, and J. Dayan, "Interacting Multiple Model Methods in Target Tracking: A Survey," *IEEE Transactions on Aerospace and Electronic Systems*, vol. 34, no. 1, pp. 103–123, 1998.

[11] R. P. S. Mahler, "Statistics 102 for Multisource-Multitarget Detection and Tracking," *IEEE Journal of Selected Topics in Signal Processing*, vol. 7, pp. 376–389, 2013.

[12] M. Liang, D. Y. Kim, and X. Kai, "Multi-Bernoulli Filter for Target Tracking with Multi-static Doppler only Measurement," *Signal Processing*, vol. 108, pp. 102–110, 2015.

[13] B. Ristic and A. Farina, "Recursive Bayesian State Estimation from Doppler-Shift Measurements," in *7th International Conference on Intelligent Sensors, Sensor Networks and Information Processing*, 2011, pp. 538–543.

[14] R. Mahler, "The Multisensor PHD Filter: I. General Solution via Multitarget Calculus," *Proceedings of SPIE - The International Society for Optical Engineering*, 05 2009.

[15] M. A. Hadi, R. Umar, M. Shoaib, M. Bilal, and K. Jamil, "Effectiveness of Deghosting Process for Multi-target Localization in Multistatic Passive Radar," in *15th European Radar Conference*, 2018, pp. 142–145.

[16] A. Samokhin, I. Ivashko, and A. Yarovoy, "Algorithm for Multiple Targets Localization and Data Association in Distributed Radar Networks," in *15th International Radar Symposium*, 2014, pp. 1–6.

[17] P. Kulmon, "Bayesian Deghosting Algorithm for Multiple Target Tracking," in *IEEE International Conference on Multisensor Fusion and Integration for Intelligent Systems*, 2020, pp. 367–372.

[18] S. Zhang and Y. Bar-Shalom, "Practical Data Association for Passive Sensors in 3D," *Journal of Advances in Information Fusion*, vol. 9, pp. 38–46, 06 2014.

[19] S. Subedi, Y. D. Zhang, M. G. Amin, and B. Himed, "Group Sparsity-Based Multi-target Tracking in Multi-static Passive Radar Systems using Doppler-only Measurements," in *IEEE Radar Conference*, 2015, pp. 880–885.

[20] G. Soldi, F. Meyer, P. Braca, and F. Hlawatsch, "Self-Tuning Algorithms for Multisensor-Multitarget Tracking using Belief Propagation," *IEEE Transactions on Signal Processing*, vol. 67, no. 15, pp. 3922–3937, 2019.

[21] S. M. Kay, *Fundamentals of Statistical Signal Processing: Estimation Theory*. USA: Prentice-Hall, Inc., 1993.

[22] S. Julier, J. Uhlmann, and H. Durrant-Whyte, "A New Method for the Nonlinear Transformation of Means and Covariances in Filters and Estimators," *IEEE Transactions on Automatic Control*, vol. 45, pp. 477 – 482, 04 2000.

[23] M. Athans, R. P. Wishner, and A. Bertolini, "Suboptimal State Estimation for Continuous-time Nonlinear Systems from Discrete Noisy Measurements," *IEEE Transactions on Automatic Control*, vol. 13, pp. 504–514, 1968.

[24] A. Doucet, S. Godsill, and C. Andrieu, "On Sequential Monte-Carlo Methods for Bayesian Filtering," *Statistics and Computing*, vol. 10, no. 3, pp. 197–208, 2000.

[25] M. Arulampalam, S. Maskell, N. Gordon, and T. Clapp, "A Tutorial on Particle Filters for Online Nonlinear/Non-Gaussian Bayesian Tracking," *IEEE Transactions on Signal Processing*, vol. 50, no. 2, pp. 174–188, 2002.

[26] S. Sruti, C. Deepti, and K. Giridhar, "Non-Parametric and Geometric Multi-Target Data Association for Distributed MIMO Radars," in *2021 IEEE Military Communications Conference*, 2021, pp. 601–606.

[27] M. A. Richards, J. Scheer, W. A. Holm, and W. L. Melvin, *Principles of Modern Radar*. Citeseer, 2010.

[28] A. Noroozi and M. A. Sebt, "Target Localization in Multistatic Passive Radar using SVD Approach for Eliminating the Nuisance Parameters," *IEEE Transactions on Aerospace and Electronic Systems*, vol. 53, no. 4, pp. 1660–1671, 2017.